Atmospheric Research 150 (2014) 143–150

Contents lists available at ScienceDirect

Atmospheric Research

journal homepage: www.elsevier.com/locate/atmos

Remote sensing of lightning by a ground-based microwave radiometer ☆

Zhenhui Wang [a,b,*], Qing Li [b], Fangchao Hu [b], Xuefen Cao [b], Yanli Chu [c]

[a] Collaborative Innovation Center on Forecast and Evaluation of Meteorological Disasters, CMA Key Laboratory for Aerosol-Cloud-Precipitation, Nanjing University of Information Science & Technology, Nanjing 210044, PR China
[b] School of Atmospheric Physics, Nanjing University of Information Science & Technology, Nanjing 210044, PR China
[c] CMA Institute of Urban Meteorological Research, Beijing 100089, PR China

ARTICLE INFO

Article history:
Received 26 May 2014
Received in revised form 7 July 2014
Accepted 8 July 2014
Available online 26 July 2014

Keywords:
Microwave radiometer
Brightness temperatures
Lightning-superheated air cylinder
Lightning remote sensing

ABSTRACT

Based on the theory of thermal radiation and its transfer in the atmosphere, the response of a ground-based microwave radiometer to a lightning-superheated cylinder in the atmosphere is studied and the theoretical expressions are given for the relationship between brightness temperatures and parameters such as distance, size, duration and temperature of the lightning-superheated cylinder. The results from simulated calculations show that it is quite possible for a lightning-superheated cylinder to be observed by a microwave radiometer working in the 50–60 GHz band with a sensitivity of 0.3 K, typically used for atmospheric temperature profiling. The brightness temperature observed with any one of the channels in the band increases as the distance between the lightning and the radiometer decreases. Lightning at a short distance would make the brightness temperature observed by the channels near to 60 GHz increase more while distant lightning would make the brightness temperature observed by the channels near to 50 GHz increase more. This feature could be used to retrieve lightning distance and features of the lightning-heated air cylinder from brightness temperature observations. One lightning observation by a ground-based radiometer, the challenge of such observations, and a theoretical analysis are presented. Additional observations are needed for more thorough exploration of this unique remote sensing capability.

1. Introduction

The electric current discharged by lightning may approach several hundred thousand amperes and the air temperature along the discharging path may be as high as thousands of Kelvins or larger (Prueitt, 1963; Ouyang et al., 2006). Abrupt heating creates a powerful explosion and sound waves. Lightning information is valuable for disaster monitoring and prediction. Current lightning detection methods include radio frequency and visible light remote sensing (Tibor, 2006). We present lightning detection by a ground-based microwave radiometer as a case study.

A microwave radiometer can detect thermal (quantum mechanical) radiation emitted by gaseous, liquid and solid matter and convert it to brightness temperatures using Planck's equations (Ulaby et al., 1981; Zhou, 1982). Ground-based microwave radiometer profilers in the 20–60 GHz range are commonly used for remote sensing of tropospheric temperature, humidity, and liquid profiles (Westwater et al., 1985; Duan and Wu, 1999; Zhu et al., 1994; Solheim et al., 1998; Güldner and Spänkuch, 2001; Westwater et al., 2004; Ware et al., 2003) and are followed with increasing interest (Ware et al., 2013; Ratnam et al., 2013; Sánchez et al., 2013; Xu et al., 2014).

☆ The work is jointly supported by National Natural Science Foundation of China (41275043, 41005005), and the Urban Meteorological Research Foundation IUMKY & UMRF201101.

* Corresponding author at: School of Atmospheric Physics, Nanjing University of Information Science & Technology, Nanjing 210044, PR China. Tel.: +86 25 58731195.
E-mail address: eiap@nuist.edu.cn (Z. Wang).

http://dx.doi.org/10.1016/j.atmosres.2014.07.009
0169-8095/

Spikes in microwave radiometer brightness temperatures were observed consistent with thermal radiation generated by lightning and propagating in accordance with microwave radiative transfer equations. We estimate microwave emission from lightning-heated air modeled in a cylindrical shape, and present simulated and actual remote sensing of such emission by a ground-based microwave radiometer. This report will hopefully stimulate further research and better understanding of lightning-induced microwave radiation.

2. Detection of microwave emission generated by lightning

According to the presentation by Dr. R. Ware of USA Radiometrics Corp., there was a microwave radiometer making brightness temperature observations at the India Space Launch Center (Trivandrum, Kerala, India) during pre-monsoon rain at around 12:20 UT (5:50 LT) on March 29, 2010. The radiometer has 14 channels in the 51–59 GHz band (Ware et al., 2013) as shown by the first 2 columns in Table 1; brightness temperature (T_b) time series in Fig. 1 show that 51.248, 51.760 and 52.280 GHz T_b's are obviously greater by 29 K, 18 K and 12 K near 12:20:20. The radiometer frequency channels are observed sequentially at 0.7 second intervals. This spike is generally correlated in time and direction with multiple lightning strokes seen by the eye.

3. Analytical model

Electron avalanches are the main constituent of electrical discharges in the atmosphere, with a duration of 1–2 ns and spectrum peak around 1 GHz (Cooray and Cooray, 2012; Petersen and Beasley, 2014). However, superheated air may also contribute to total lightning-induced microwave emission. Though the discharging path of a cloud-to-ground lightning may propagate in any pattern, it can be simplified as a vertical cylinder for distant observations and therefore the lightning superheated area is considered as a vertical, elliptical cylinder. Suppose the radiometer is pointing at the direction (r) of the lightning, as shown in Fig. 2, to receive the thermal radiance from the superheated air cylinder with a radial diameter D_R and a cross-range diameter D_L. The beam width of the radiometer antenna at 51–59 GHz varies with frequency from 2.3° to 2.7° and we take $\alpha = 2.5° = 0.044$ rad on average, therefore the cross-section diameter of the antenna beam is $D_A = \alpha r \approx 44$ m at $r = 1$ km and $D_A \approx 440$ m at $r = 10$ km. In order to make it easy to observe lightning from a distance, the antenna should be adjusted to low elevation. And it is better to hold $D_A < D_L$ so that the beam is full of the heated air at the distance r otherwise corrections as discussed in Section 5.3 of the paper must be performed. The temperature inside the superheated air cylinder may not be uniform (Prueitt, 1963) but for total radiance simulation the beam intersection area is assumed to be uniform.

Suppose that the volumetric absorption coefficient at distance r is $k_a(r)$ (Liebe et al., 1992) and the influence of scattering on microwave radiance transfer is negligible, the transmittance in the range $[0, r)$ according to Beer's law would be

$$\tau(r) = \exp\left\{-\int_0^r k_a(r)dr\right\} \tag{1}$$

The radiance measured by a radiometer in terms of brightness temperature is defined by radiative transfer equation (Ulaby et al., 1981; Yao and Chen, 2005; Zhang and Wang, 1995)

$$T_b(0) = T_{b\infty}\tau(\infty) + \int_0^\infty T(r)W(r)dr \tag{2}$$

where $T_{b\infty}$ is the background brightness temperature from the out-space, $\tau(\infty)$ is the transmittance from the out-space to the radiometer, $T(r)$ the temperature of the air cylinder at distance r, and

$$W(r) = -\frac{d\tau(r)}{dr} = \tau(r)k_a(r) \tag{3}$$

is called as weighting function. $k_a(r)$, $\tau(r)$ and $W(r)$ for the 4 typical channels are calculated for the case of standard atmosphere at 15° elevation. The 3rd column of Table 1 lists the values of $k_a(r)$ at $r = 0$, i.e., $k_a(r = 0)$ and Fig. 3 gives the profiles of $\tau(r)$ and $W(r)$. It can be seen that:

(1) $k_a(r)$ increases as frequency increases for a given distance, but $k_a(r)$ changes little as r increases for a

Table 1
Radiometer channel frequencies, absorption coefficient (k_a) of a standard atmosphere at sea level, apparent emissivity (ε), and the simulated brightness temperature in the case of $\alpha = 1°$, $R_1 = 3$ km, $\Delta T = 10{,}000$ K, $D_R = 60$ m, and $D_L = 60$ m.

Channel	Freq. (GHz)	k_a (Np/km)	ε	T_b (K) without lightning	ΔT_b (K) because of lightning	ΔT_b (K) after correction for $\alpha = 2.5°$
1	51.248	0.156	0.009	90.7	46.6	21.2
2	51.760	0.184	0.011	105.1	51.8	23.5
3	52.280	0.255	0.015	124.8	58.0	26.4
4	52.804	0.287	0.017	151.0	63.5	28.9
5	53.336	0.380	0.023	183.5	**66.3**	30.1
6	53.848	0.508	0.030	216.8	62.8	28.5
7	54.400	0.704	0.041	248.3	50.4	22.9
8	54.940	0.962	0.056	268.8	33.0	15.0
9	55.500	1.298	0.075	279.2	16.6	7.5
10	56.020	1.657	0.095	282.9	7.3	3.3
11	56.660	2.105	0.119	284.4	2.5	1.1
12	57.288	2.500	0.139	285.0	0.9	0.4
13	57.964	2.859	0.158	285.4	0.3	0.1
14	58.800	3.183	0.174	285.6	0.1	0.0

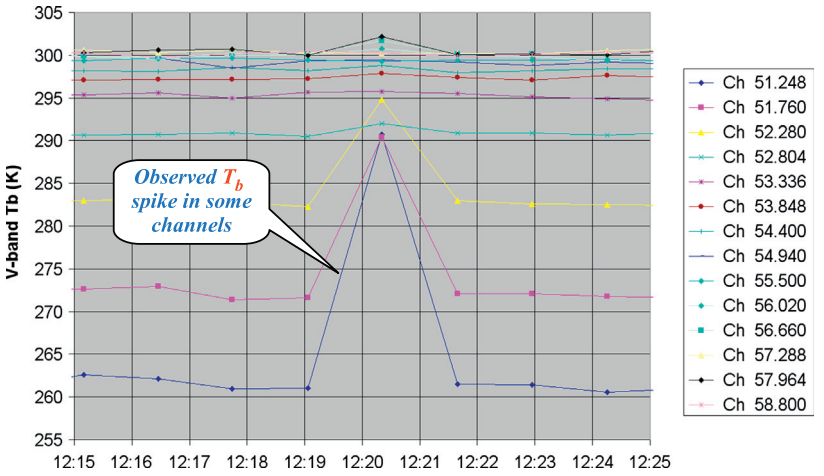

Fig. 1. Time series of brightness temperatures observed by a microwave radiometer installed at India Space Launch Center, Trivandrum, Kerala, India, during 12:15–12:25 UT(5:45–5:55 LT) on Mar. 29, 2010 at 15° elevation.
(From slides presented in November, 2010, at Nanjing University of Information Science and Technology by R. Ware, Radiometrics Corporation).

certain frequency because the elevation is only 15°. Therefore $k_a(r)$ is approximately independent of distance and is abbreviated as k_a hereinafter;

(2) transmittance at $r = 0$ is always 1 but the weighting function at $r = 0$ is different for different frequencies. This is because $W(r = 0) = k_a$, i.e., for higher frequencies such as 57.964 GHz, atmospheric absorption is strong and $W(r = 0)$ would be greater than for the lower frequencies such as 51.248 GHz at which the atmospheric absorption is weak;

(3) both $\tau(r)$ and $W(r)$ decrease as r increases but

(4) the decreasing rates with respect to r are different at different distances. For example, $W(r)$ at $r = 0$ km are 1.298 and 0.380 for 55.500 and 53.336 GHz, respectively, while at $r = 3$ km, $W(r)$ decreases down to 0.112 for 53.336 GHz and to less than 0.029 for 55.500 GHz. Both the transmittance $\tau(r)$ and the weight $W(r)$ for high frequency such as 57.964 GHz decrease faster than those for low frequency such as 51.248 GHz because of the difference in absorption coefficient. This feature makes it possible to determine lightning distance with a multi-channel radiometer as discussed in Section 5.

Let the distance from lightning-heated cylinder to the radiometer be R_1,as shown in Fig. 2, and radial diameter of the cylinder is $D_R = R_2 - R_1$. Let T^+ be the temperature inside the range (R_1, R_2) after discharging. It would become

$$T^+ = T(r) + \Delta T(r) \tag{4}$$

i.e., the temperature is increased by $\Delta T(r)$ due to lightning. Considering that the increased radiant energy because of the lightning is contributed only by the heated cylinder, the increment in brightness temperature measured by the radiometer, according to Eq. (1), should be

$$\Delta T_b = \int_{R_1}^{R_2} \Delta T(r) W(r) dr = \Delta T(R_1) * \int_{R_1}^{R_2} W(r) dr. \tag{5}$$

The equation is further alternated as

$$\Delta T_b = \Delta T(R_1) * \overline{W(R_1)} * D_R \tag{6}$$

where $\overline{W(R_1)}$ is the mean value of $W(r)$ in the range (R_1, R_2). This formula implies that the response of the radiometer to

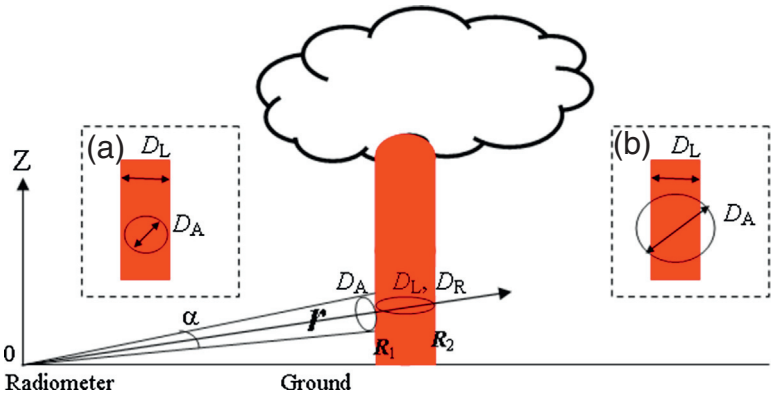

Fig. 2. Model for ground-based radiometer observation of a lightning-superheated cylinder in the atmosphere. Two dashed-line squares show the concept of beam-filling in the cases of full filling and partial filling.

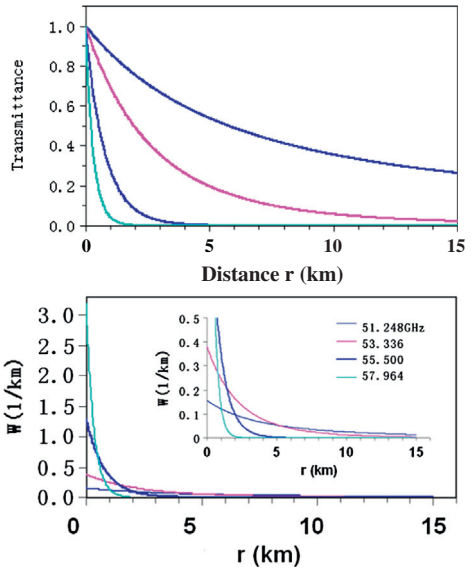

Fig. 3. Transmittance (upper) and weighting functions (lower) for the 4 typical channels of the microwave radiometer when elevation is 15° (inset vertical axis = 0.5 km^{-1}).

lightning heating is proportional to the temperature increment of the air cylinder and its radial diameter with the mean value of $W(r)$ in the cylinder as the proportional coefficient. Estimation of ΔT_b can be directly completed with Eq. (5) since $W(r)$ has been given by Fig. 3.

On the other hand, insert $W(r) = -\frac{d\tau(r)}{dr}$ as defined by Eq. (3) into Eq. (5) and makes use of the relationship among transmittance, absorption and emissivity (Zhang and Wang, 1995), and we have

$$\Delta T_b = \Delta T(R_1) * (\tau(R_1) - \tau(R_2)) = \varepsilon * \Delta T(R_1) * \tau(R_1) \tag{7}$$

where

$$\varepsilon = 1 - \tau(R_2)/\tau(R_1). \tag{8}$$

ε is the apparent emissivity of the air cylinder. Eq. (7) implies that the response of the radiometer to lightning heating is proportional to both the temperature increment of the air cylinder and the transmittance from the cylinder to the radiometer. The proportional coefficient is the apparent emissivity of the cylinder. Therefore, for the purpose of response estimation, the cylinder can be taken as a radiant flat at temperature $\Delta T(R_1)$ with an apparent emissivity determined by Eq. (8).

Note that $0 \le \varepsilon \le 1$ and according to Eqs. (1) and (8), one has

$$\varepsilon = 1 - \exp(-k_a D_R) \tag{9}$$

i.e., the value of ε depends on the radial diameter of the cylinder and its internal nature. A thick cylinder has a large emissivity at high frequency channel. The 4th column of Table 1 lists the values of emissivity for $D_R = 60$ m computed in the condition that k_a has been given in the 3rd column for Standard Atmosphere. It can be seen that ε is small in general and less than 0.2 at the highest frequency. After discharging, the cylinder is at the extreme temperature, pressure, and ionization state, k_a and ε for the cylinder might change. The difference would add some uncertainty to the estimation of ΔT from ΔTb according to Eq. (7). Fortunately, both ε and ΔT are all lightning-dependent and are included as a product in Eq. (7). Therefore, take ε as a parameter independent of lightning and ΔT retrieved from Eq. (7) would be indicative of lightning radiance rather than physical temperature. That is, if ε after lightning increases by a percentage, retrieved ΔT must be adjusted according to the percentage in order to obtain the increase of physical temperature. Therefore it is assumed that k_a and ε inside the cylinder are reference constants a in the following discussion.

4. Parameter selection for simulation and analysis

The response of radiometer to a lightning-heated air cylinder is different at different frequencies because they are characterized by different transmittance and weighting functions as shown by Fig. 3. This can be quantitatively verified as the following simulative calculation.

In the simulation, let the antenna elevation be 15°, beam width $\alpha = 1°$, i.e., $D_A \approx 51$ m at $r = 3$ km. A lightning-heated air cylinder being observed by the radiometer is at the distance $R_1 = 3$ km and the cylinder diameter is 60 m (i.e., $D_R = D_L =$ 60 m and $D_L \ge D_A$) as shown by the sub-panel embedded in the left half of Fig. 2. Suppose the air from the cylinder to the radiometer is the same as the Standard Atmosphere and only the temperature inside the cylinder increases by $\Delta T = 10{,}000$ K as shown in Fig. 4.

The result from the simulation for $R_1 = 3$ km, $\Delta T = 10{,}000$ K and $D_R = 60$ m, is given in Columns 5 and 6 of Table 1. Column 5 lists T_b, the brightness temperatures observed without the existence of the lightning-heated air cylinder and Column 6 lists ΔT_b, the response of the radiometer to the lightning-heated air cylinder. One can see that:

(1) brightness temperatures are all increased and 12 channels of the 14 increase by more than 0.5 K. Since the nominal sensitivity of operational microwave radiometer is 0.3 K rms, most channels can detect signals greater than 1 K from the lightning-heated air cylinder featured by $\Delta T = 10{,}000$ K and $D_R = 60$ m at $R_1 = 3$ km;
(2) brightness temperature at 53.336 GHz increases by 66.3 K, as shown by the bold type in column 6 for Channel 5, which is the largest amplitude relative to other channels. The increased amplitude decreases as the frequency difference of a specified channel from 53.336 GHz increases. The response of 58.800 GHz channel is negligible because both the transmittance and weighting are nearly 0 at $R_1 = 3$ km as shown in Fig. 3.

5. Further analysis on the relationship between ΔT_b and lightning parameters

5.1. Relationship between ΔT_b and distance R_1

Fig. 5 gives ΔT_b's for 14 frequencies as a function of distance R_1.

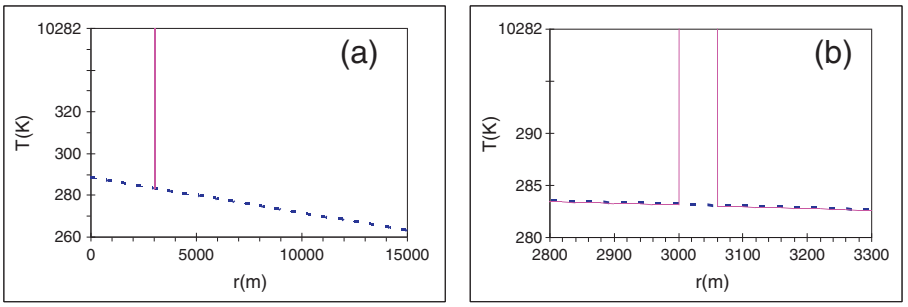

Fig. 4. Air temperature distribution as a function of distance from the radiometer in the case of 15°, $R_1 = 3$ km, $\Delta T = 10{,}000$ K, and $D_R = 60$ m. The dashed line is the temperature following the standard atmosphere and the solid line is pulsed because of the lightning-superheating. The right panel is the same as the left but enlarged to make the pulse outstanding.

It can be seen that

(1) lightning at a shorter distance promotes higher frequency channels to make an outstanding response. This is because ε in Eq. (7) is greater at higher frequency;
(2) brightness temperature increment at any given frequency decreases as distance increases. This is because $\tau(R_1)$ in Eq. (7) decreases as R_1 increases as shown in Eq. (1);
(3) brightness temperature increments at higher frequency decrease faster as R_1 increases, implying that the maximum of ΔT_b at a certain distance corresponds to a certain channel. For instance, the maximum of ΔT_b at $R_1 \approx 1.0$ km is roughly 250 K corresponding to 57.288 GHz channel, the maximum of ΔT_b at $R_1 \approx 2.0$ km is a little bit more than 100 K corresponding to 54.400 GHz channel, the maximum of ΔT_b at $R_1 \approx 3.0$ km is approximately 60 K corresponding to 53.336 GHz channel, the maximum of ΔT_b at $R_1 \approx 6.0$ km is about 30 K corresponding to 52.804 GHz channel, the maximum of ΔT_b at $R_1 \approx 10.0$ km is close to 15 K corresponding to 52.280 GHz channel, and the maximum of ΔT_b at $R_1 \approx 15.0$ km is about 8 K corresponding to 51.248 GHz channel. This feature makes lightning distance estimates possible using simultaneous multi-channel radiometer observations.

5.2. Relationship between ΔT_b and radial diameter D_R

Under the condition of $D_L > D_A$, the decrease of cylinder radial diameter leads to the decrease of ΔT_b for any channel as shown by Eq. (5). Fig. 6 gives the calculated results in the condition which is the same as in Fig. 5 but for $D_R = 20$ m (Chen, 2006). The decrease of cylinder radial diameter is equivalent to the decrease of ε according to Eq. (9) and further the decrease of ΔT_b according to Eq. (7). So the brightness temperature increment in Fig. 6 is less than that in Fig. 5 but the 3 points derived from Fig. 5 are all quantitatively applicable to Fig. 6.

5.3. Relationship between ΔT_b and antenna beam width α

Antenna beam width at 51–59 GHz for T_b observations is roughly 2.5° rather than 1°. This would lead to "$D_L < D_A$", especially if the lightning-heated cylinder is quite small and distant. That is, the cylinder cannot fully fill the cross-section of the beam as shown by the sub-panel embedded in the right half

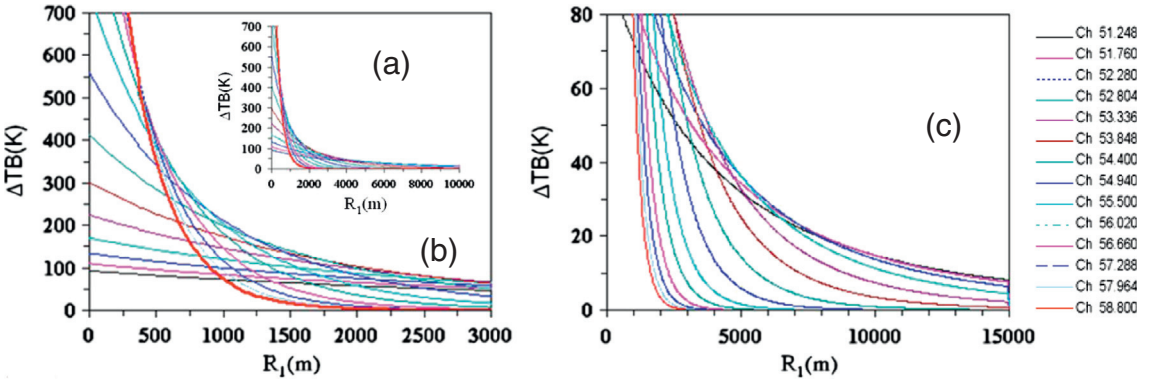

Fig. 5. Brightness temperature increment at 14 frequencies as a function of distance in the case of $\Delta T = 10{,}000$ K and $D_R = 60$ m. (a) General feature, (b) zoom in for short distance, (c) zoom in for long distance (inset horizontal axis = 10,000 m).

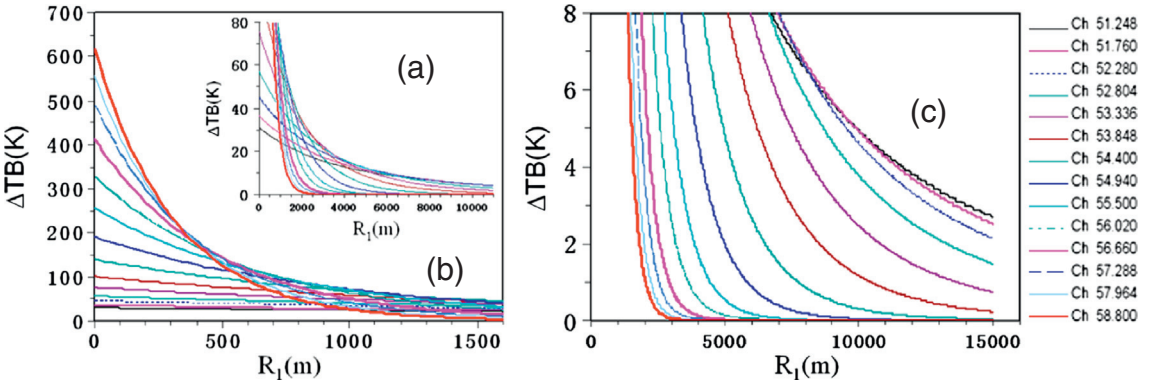

Fig. 6. The same as Fig. 5 but for $D_R = 20$ m.

of Fig. 2. In this case, the response estimated with Eq. (5) should be corrected for partial beam filling, named as "partial beam filling correction". Knowing the correction factor denoted by c_1, one has

$$\Delta T_b^c = c_1 * \Delta T_b \tag{10}$$

where $c_1 \in [0,1]$. The factor should be the area ratio as shown by the sub-panel embedded in the right half of Fig. 2 but an approximation is the following

$$c_1 = \begin{cases} D_L/D_A & \text{for } D_L/D_A<1 \\ 1 & \text{for the others} \end{cases}.$$

Since $D_A = \alpha R_1$, then

$$c_1 = \begin{cases} D_L/\alpha R_1 & \text{for } D_L/\alpha R_1<1 \\ 1 & \text{for the others} \end{cases}. \tag{11}$$

For the case $\alpha = 2.5° = 0.044$ rad, $R_1 = 3$ km, $D_A \approx 132$ m, and $c_1 = 0.455$ for $D_L = 60$ m. Substitute this into Eq. (10), the ΔT_b after correction is given in the last column of Table 1. One can see that ΔT_b (K) after correction for beam filling has been decreased but still most of the channels show a large response. Nevertheless, it is still hoped that antenna beam width for the purpose of monitoring lightning be as narrow as possible.

The scale of D_L is of course very important in this issue. Based on optical observations with high-speed camera system, the spatial size of an individual return stroke is on the order of 10 m, the width of a band-type flash can be greater than 10 m (Chen, 2006), and the scale of a complete lightning stroke including a series of return strokes and lasting for tens to hundreds of milliseconds may be tens and even nearly 100 m. If we take these as the scale of D_L, it is really possible for c_1 in Eq. (10) to be close to 1 under certain conditions.

5.4. Relationship between ΔT_b and integration time

Let D_{TA} be defined as the effective radiometer sky-observation time (including noise diode calibration and switching times). In this case D_{TA} = ~700 ms. Let D_{TL} denote the duration time of a super-heated air cylinder. In case $D_{TL} \geq D_{TA}$ and D_{TA} falls within the D_{TL} time frame, ΔT_b simulated can be directly compared with ΔT_b observation. Otherwise it must be corrected for $D_{TL} < D_{TA}$, as the following

$$\Delta T_b{}^c = c_2 * \Delta T_b \tag{12}$$

which is called "partial time filling correction". The correction factor is determined by

$$c_2 = \begin{cases} D_{TL}/D_{TA} & \text{for } D_{TL}<D_{TA} \\ 1 & \text{for } D_{TL} \geq D_{TA} \end{cases}. \tag{13}$$

The value of D_{TL} depends on duration of flash, thickness of super-heated air cylinder, wind speed and so on. Duration time of a long stroke is typically more than 2 ms and less than 1 s (Wang et al., 2013). Therefore c_2 may be any value in the range [0,1]. To benefit the monitoring of lightning, integration time should be as short as possible.

Combining together the two corrections above and putting them into Eq. (7), one obtains the simulated response after correction

$$\Delta T_b = \tau(R_1) * c_1 * c_2 * \varepsilon * \Delta T(R_1). \tag{14}$$

Putting Eqs. (1), (9), (11) and (13) into Eq. (14), simplifying $\Delta T(R_1)$ as ΔT, and foot-noting frequency-dependent parameters with subscript i, one has

$$\Delta T_{bi} = \frac{D_{TL}}{\alpha D_{TA}}(1-\exp\{-k_{ai}D_R\})\exp\{-k_{ai}R_1\}\frac{D_L}{R_1}\Delta T. \tag{15}$$

If $k_a D_R$ is small enough, one has the following approximation

$$\Delta T_{bi} = \frac{D_{TL}}{\alpha D_{TA}} k_{ai} \exp\{-k_{ai}R_1\}\frac{D_R D_L}{R_1}\Delta T. \tag{16}$$

It can be seen that

(1) The response of brightness temperature to lightning is proportional to the increment of cylinder temperature, the duration time and the area of the cylinder cross-section, and inversely proportional to distance in case $D_{TL} < D_{TA}$ and $D_L < D_A$.

(2) The distance can be solved from the ratio of two responses obtained with 2 frequencies according to

$$R_1 = \ln\left(\frac{\Delta T_{bi}}{\Delta T_{bj}}\frac{k_{aj}}{k_{ai}}\right)\Big/\left(k_{aj}-k_{ai}\right) \quad (17)$$

and the product of the increment of cylinder temperature, the duration time and the area of the cylinder cross-section such as

$$\mathrm{B} = D_{\mathrm{TL}}D_{\mathrm{R}}D_{\mathrm{L}}\Delta\mathrm{T} = \Delta T_{bi}\alpha D_{TA}R_1/(k_{ai}\exp\{-k_{ai}R_1\}) \quad (18)$$

can be estimated and used as a parameter to indicate the intensity of lightning.

6. On the possibility to detect lightning as seen in Fig. 1

The preliminary analysis above shows that it is really possible for a ground-based microwave radiometer to detect lightning and its observations of brightness temperature in 51–59 GHz can be used to estimate the distance and features of the lightning-heated air cylinder, especially if the brightness temperature dynamic range of the radiometer is wide enough, the antenna of the radiometer is pointing toward the lightning and the beam width and integration time are all adequate.

In the case given in Fig. 1, 29, 18 and 12 K spikes are seen at 51.248, 51.760 and 52.280 GHz respectively at 12:20:20. Since the frequencies are the lowest, the position of the lightning mentioned in Section 1 must be quite far and intense. Consider $D_{TA} = 1$ s, $\alpha = 2.5^\circ = 0.044$ rad, and suppose that the value of k_a in Table 1 is tripled for the observation site (considering that the water vapor content in tropical area may be 3 times that for standard atmosphere), and the increments of 29 and 18 K for Channels 51.248 and 51.760 GHz are substituted into Eqs. (17) and (18), we can obtain that $R_1 = 7.64$ km and $\mathrm{B} = D_{TL}D_RD_L\Delta\mathrm{T} = 744$ K km^2 s. One of the possible condition for this result is $D_{TL} = 1$ s, $D_RD_L = 60$ m*300 m $= 0.018$ km^2 ($D_A = \alpha R_1 = 0.044$*7.64 $= 336$ m, $D_L \approx D_A$) and $\Delta T \approx 4.1 * 10^4$ K, implying that the cylinder must be the result of a long stroke or a series of return strokes.

We really want to make verification for this judgment but unfortunately data needed are not available. It is therefore suggested that, in case the experiment for verification of this kind is performed in the future, lightning distance should be obtained with lightning locating system such as IMPACT or SAFIR. Of course, instruments for detecting parameters like ΔT, D_R, D_L and D_{TL} are also needed if available. This is just the innovative sense of the study in order to use a microwave radiometer to monitor lightning.

7. Conclusion

Emissions from a super-heated air cylinder generated by lightning can be observed with a ground-based microwave radiometer currently used for atmospheric temperature, humidity and liquid profiling. Simulated and preliminary observation analysis shows the following:

(1) The T_b response of the radiometer is proportional to both the increment of temperature in the discharging area and the atmospheric transmittance to the radiometer, and the proportional factor is the emissivity of the lightning-heated air cylinder.
(2) The T_b response at any frequency associated with the radiometer channels is inversely proportional to the distance between the radiometer and the cylinder.
(3) The emissivity of the lightning-heated air cylinder is greater at higher frequency than at lower frequency. This implies that lightning at a shorter distance results in a higher frequency channel to make an outstanding response while distant lightning leads a lower frequency channel to make an outstanding response.
(4) Derived from points (2) and (3) above is that there is a maximum T_b response for a certain distance at a certain frequency. Therefore, the distance and features of the lightning-heated air cylinder can be estimated from T_b observations with the radiometer.
(5) To benefit lightning monitoring with a microwave radiometer, the beam width should be as narrow as possible and the integration time as short as possible. In the case of distance $R_1 = 3$ km, lightning heating $\Delta T = 10{,}000$ K and cylinder diameter $D_R = D_L = 60$ m, even "partial filling" correction is 1% (i.e., $c_1 * c_2 = 0.01$), there are still a few lower-frequency channels to respond by more than 0.5 K. But the difficulty for a ground-based microwave radiometer to observe lightning is that the radiometer does not know in advance the direction of possible discharge.

It has been assumed in the paper that the apparent emissivity of the lightning-heated air cylinder for thermal radiation is the same as before lightning. This assumption does not affect the ability to discern range according to Eq. (17) since the frequency dependence of absorption outside the cylinder is not altered but may add some uncertainty to the estimation of ΔT according to Eq. (18).

As it is said that "Tossing out a brick to get a jade gem", the paper serves as a modest spur to stimulate additional research on lightning monitoring with microwave radiometer in order to understand the magnitude of heating by lightning at a specific distance, with a specific strength and microwave radiance. And even more, the radiometer is sensitive not only to thermal emission from lightning heated air, but also to electromagnetic emission generated directly from the lightning electric pulse, as described in the articles by Krider (2003) and Gurevich et al. (1992). This should be taken into account for accurate retrievals of lightning parameters from microwave radiometer observations.

Acknowledgment

We thank Dr. R. Ware (Radiometrics Corporation, USA) for stimulating us to start this study during his November 2010 presentation at Nanjing University of Information Science and Technology and his later continuous suggestions and modifications to this paper and Dr. Tan Yongbo of NUIST/Department of Lightning Sci. & Technology for his comments on the manuscript.

References

Chen, W., 2006. The Principle of Lightning, 2nd ed. Meteorological Press, Beijing, pp. 1–419 (in Chinese).

Cooray, V., Cooray, G., 2012. Electromagnetic radiation field of an electron avalanche. Atmos. Res. 117, 18–27.
Duan, Y., Wu, Z., 1999. Monitoring the distribution characteristics of liquid and vapour water content in the atmosphere using ground-based remote sensing. Q. J. Appl. Meteorol. 10 (1), 34–40 (in Chinese).
Güldner, J., Spänkuch, D., 2001. Remote sensing of the thermodynamic state of the atmospheric boundary layer by ground-based microwave radiometry. J. Atmos. Ocean. Technol. 18, 925–933.
Gurevich, A.V., Milikh, G.M., Roussel-Dupre, R., 1992. Runaway electron mechanism of air breakdown and preconditioning during a thunderstorm. Phys. Lett. A 165, 463–468.
Krider, Philip E., 2003. Deciphering the energetics of lightning. Science 299, 669–670.
Liebe, H.J., Rosenkranz, P.W., Hufford, G.A., 1992. Atmospheric 60-GHz oxygen spectrum: new laboratory measurements and line parameters. J. Quant. Spectrosc. Radiat. Transf. 48, 629–643.
Ouyang, Y., Yuan, P., Jia, X., 2006. Multiple-line method used to calculate lightning channel temperature. J. Northwest Norm. Univ. (Nat. Sci.) 42 (3), 49–53 (in Chinese).
Petersen, D., Beasley, W., 2014. Microwave radio emissions of negative cloud-to-ground lightning flashes. Atmos. Res. 135–136, 314–321.
Prueitt, M.L., 1963. The excitation temperature of lightning. Geophys. Res. 68, 803–811.
Ratnam, M., Venkat, Y. Durga, Santhi, M., Rajeevan, S. Vijaya, Rao, Bhaskara, 2013. Diurnal variability of stability indices observed using radiosonde observations over a tropical station: comparison with microwave radiometer measurements. Atmos. Res. 124, 21–33.
Sánchez, J.L., Posada, R., García-Ortega, E., López, L., Marcos, J.L., 2013. A method to improve the accuracy of continuous measuring of vertical profiles of temperature and water vapor density by means of a ground-based microwave radiometer. Atmos. Res. 122, 43–54.
Solheim, F., Godwin, J., Westwater, E., Han, Y., Keihm, S., Marsh, K., Ware, R., 1998. Radiometric profiling of temperature, water vapor, and cloud liquid water using various inversion methods. Radio Sci. 33 (2), 393–404.
Tibor, Horv, 2006. Understanding Lightning and Lightning Protection: A Multimedia Teaching Guide. John Wiley, pp. 1–220.
Ulaby, F.T., Moore, R.K., Fung, A.K., 1981. Microwave remote sensing. Active and Passive, vol. 1. Addison-Wesley Publishing Company [M]. Advanced Book Program/World Science Division, Reading, MA, USA, pp. 1–456.
Wang, Z., Li, X., Guo, F., Shi, G., 2013. 101 Topics on Lightning and its Prediction, Revised ed. Meteorological Press, Beijing, pp. 1–284.
Ware, R., Solheim, F., Carpenter, R., Güldner, J., Liljegren, J., Nehrkorn, T., Vandenberghe, F., 2003. A multi-channel radiometric profiler of temperature, humidity and cloud liquid. Radio Sci. 38, 8079–8091.
Ware, R., Cimini, D., Campos, E., Giuliani, G., Albers, S., Nelson, M., Koch, S.E., Joe, P., Cober, S., 2013. Thermodynamic and liquid profiling during the 2010 Winter Olympics. Atmos. Res. 132, 278–290.
Westwater, E.R., Wang, Zhenhui, Grody, N.C., McMillin, L.M., 1985. Remote sensing of temperature profiles from a combination of observations from the satellite-based microwave sounding unit and the ground-based profiler. J. Atmos. Ocean. Technol. 2, 97–109.
Westwater, E., Crewell, S., Matzler, C., 2004. A review of surface-based microwave and millimeter-wave radiometric remote sensing of the troposphere. Radio Science Bulletin, No. 310, pp. 59–80 (Sept.).
Xu, Guirong, Ware, Randolph (Stick), Zhang, Wengang, Feng, Guangliu, Liao, Kewen, Liu, Yibing, 2014. Effect of off-zenith observations on reducing the impact of precipitation on ground-based microwave radiometer measurement accuracy. Atmos. Res. 140-141, 85–94.
Yao, Z., Chen, H., 2005. Analysis of the remote sensing of atmospheric temperature profiles using the seven channel microwave radiometer. Sci. Meteorol. Sin. 25 (2), 133–141 (in Chinese).
Zhang, P., Wang, Z., 1995. Fundamentals of Atmospheric Microwave Remote Sensing. Meteorological Press, Beijing, pp. 1–412 (in Chinese).
Zhou, Xiuji, 1982. Microwave Radiation in the Atmosphere and the Principle for Its Remote Sensing. Science Press, Beijing, pp. 1–178 (in Chinese).
Zhu, Y., Hu, C., Zhen, J., Zhao, B., 1994. The role of microwave radiometer in weather modification research. Acta Sci. Nat. Univ. Pekin. 30 (5), 597–606 (in Chinese).